Narrowband oscillations from asynchronous neural activity

Stephen V. Gliske,[1,*] Eugene Lim,[2] Katherine A. Holman,[3] William C. Stacey,[1,4] and Christian G. Fink[2,5]

[1] *Dept. of Neurology, University of Michigan*
[2] *Dept. of Physics, Ohio Wesleyan University*
[3] *Dept. of Physics, Towson University*
[4] *Dept. of Biomedical Engineering, University of Michigan*
[5] *Neuroscience Program, Ohio Wesleyan University*

(Dated: December 8, 2015)

We investigate the possibility that narrowband oscillations may emerge from completely asynchronous, independent neural firing. We find that a population of asynchronous neurons may produce narrowband oscillations if each neuron fires quasi-periodically, and we deduce bounds on the degree of variability in neural spike-timing which will permit the emergence of such oscillations. These results suggest a novel mechanism of neural rhythmogenesis, and they help to explain recent experimental reports of large-amplitude local field potential oscillations in the absence of neural spike-timing synchrony. Simply put, although synchrony can produce oscillations, oscillations do not always imply the existence of synchrony.

arXiv:1512.01622v1 [q-bio.NC] 5 Dec 2015

Neural rhythms, as observed in electroencephalogram (EEG) and local field potential (LFP) recordings, are associated with various brain functions and are generated through manifold mechanisms [1]. One interesting feature of neural rhythms is that they are often observed in conjunction with irregular spiking of individual neurons [2]. This phenomenon has previously been explained by analyzing the interplay between excitatory and inhibitory synaptic time scales and feedback loops [3], stochastic resonance [4], or correlations in stochastic input [5]. However, all of these mechanisms will produce non-trivial levels of spike-timing synchrony within a population of neurons, and recent experimental studies have demonstrated examples of epileptic seizures which feature narrowband LFP oscillations in the absence of population synchrony [6, 7].

In the present work we demonstrate that narrowband oscillations may emerge from a population of neurons that fire asynchronously, independently, and stochastically. This may be accomplished if the neurons naturally fire with some rhythmicity and with similar average frequencies, conditions which may plausibly be met if a population of neurons receives similar intensity of input and shares similar biophysical parameters. This work therefore proposes a novel and general mechanism for the generation of brain rhythms. We also derive bounds on the levels of spike-timing heterogeneity which allow for the emergence of such rhythms.

As a toy example, consider a situation in which a population of N neurons fire with the same frequency f_0, but with uniformly random phase. The contribution to the LFP by any one neuron, $g(t)$, is well approximated as the convolution of a periodic train of delta functions with a kernel waveform (representing the voltage trace of an individual action potential, for example). The Fourier transform of this signal, $G(f)$, will feature peaks at f_0 and its harmonics, with an amplitude of zero at all other frequencies. The LFP will then be the superposition of N randomly-shifted versions of $g(t)$, $g_N(t) = \sum_{j=1}^{N} g(t - t_{0,j})$, with $t_{0,j} \sim \text{unif}(0, \frac{1}{f_0})$. The Fourier transform of the LFP is then $G_N(f) = \left[\sum_{j=1}^{N} e^{i\theta_j}\right] G(f)$, where $\theta_j = -2\pi f t_{0,j}$. The energy spectral density can be determined by defining $A = \sum_{j=1}^{N} e^{i\theta_j}$ and computing its expected squared amplitude:

$$E\left\{|A(f)|^2\right\} = \int_0^{1/f_0} dt_{0,1} \ldots dt_{0,N}\ p(t_{0,1})\ \ldots\ p(t_{0,N})\ |A(f)|^2$$

$$= \left(\frac{-f_0}{2\pi f}\right)^N \int_0^{2\pi f/f_0} d\theta_1 \ldots d\theta_N \left(\sum_{j=1}^{N} e^{i\theta_j}\right)\left(\sum_{k=1}^{N} e^{-i\theta_k}\right)$$

$$= N + N(N-1)\,\text{sinc}^2\left(\frac{\pi f}{f_0}\right)$$

Combining this result with the fact that $G_N(f) = 0$ for all non-harmonic frequencies, the energy spectral density is

$$E\left\{|G_N(f)|^2\right\} = \begin{cases} N|G(f)|^2, & f = nf_0\ (n = 1, 2, 3...) \\ 0, & \text{otherwise} \end{cases} \tag{1}$$

This toy model therefore suggests the possibility of narrowband collective oscillations emerging from asynchronous neural activity. This example is analogous to the fact that incoherent light waves do not produce completely destructive interference, but superimpose with an intensity that scales linearly with the number of waves.

Of course, individual neurons do not spike perfectly periodically, nor do they share the same intrinsic frequency across a population. We therefore introduce a model of asynchronous, independent, and stochastic neural activity which takes both of these sources of spike-time variability into account. Specifically, we consider a superposition of renewal processes (which is not itself a renewal

process [8]) in which the inter-event interval (IEI) density of neuron i is given by

$$p_0(\tau^{(i)}|\mu_i,\sigma_{\text{jit}}) = \frac{1}{\sigma_{\text{jit}}\sqrt{2\pi}} \exp\left(\frac{-(\tau^{(i)}-\mu_i)^2}{2\sigma_{\text{jit}}^2}\right), \quad (2)$$

with the parameter μ_i also being normally distributed, drawn from $\mathcal{N}(\mu_0,\sigma_\mu)$, and σ_{jit} being a fixed model parameter. Therefore σ_μ determines the variability in intrinsic frequency for the entire population, and σ_{jit} quantifies the degree of "jitter" from one event to the next for a single neuron. The mean population frequency is set by μ_0. (Note that while this technically permits negative IEI values, this will occur very rarely as long as σ_μ and σ_{jit} are kept sufficiently small with respect to μ_0.)

We assume all events generate either an action potential (AP) or post-synaptic potential (PSP) voltage waveform, so that the overall LFP is computed as the convolution of the waveform with the event trains generated by Eq. 2, summed over all neurons. Our goal is to compute the expected energy spectral density of this model LFP. Since the energy spectrum of such a convolution is the product of the energy spectra of the fixed waveform and the event train, we initially focus on just the spectrum of the event train.

Let each neuron have event times given by $f^{(k)}(t)$, with the population level spike train being $f_T(t) = \sum_{j=1}^{N_C} f^{(j)}(t)$ and N_C being the number of cells. The energy spectral density of this aggregate event train is then given by the functional integral

$$\begin{aligned}\mathbb{E}_{p(f)}\left[|\mathcal{F}[f_T]|^2\right] &= \int df_T\ p(f_T)\,|\mathcal{F}[f_T]|^2\,, \\ &= \int \left[\prod_j df^{(j)}\ p\left(f^{(j)}\right)\right] \left|\sum_{k=1}^{N_C}\mathcal{F}\left[f^{(k)}\right]\right|^2.\end{aligned}$$

Assuming event trains are independent from cell to cell, and that all cells' event trains are drawn from the same family of distributions, this simplifies to

$$\begin{aligned}\mathbb{E}_{p(f)}\left[|\mathcal{F}[f_T]|^2\right] &= N_C \int df\ p(f)\,|\mathcal{F}[f]|^2 \quad (3)\\ &\quad + \frac{1}{2}N_C(N_C-1)\left|\int df\ p(f)\,\mathcal{F}[f]\right|^2.\end{aligned}$$

In general, since each event train is parameterized by a discrete set of event times t_k, the integration measures are $\int df\ p(f) = \int d\boldsymbol{\theta} p(\boldsymbol{\theta}) \prod_k dt_k\ p_k(t_k|\boldsymbol{\theta})$, where $\boldsymbol{\theta}$ represents any additional model parameters on which the pdfs are conditioned. The Fourier transform of f and its magnitude are then

$$\mathcal{F}[f] = \frac{1}{\sqrt{2\pi}}\frac{1}{N_S}\sum_k e^{-i\omega t_k}, \quad (4)$$

$$|\mathcal{F}[f]|^2 = \frac{1}{2\pi}\frac{1}{N_S^2}\sum_{k,\ell} e^{-i\omega(t_k-t_\ell)}. \quad (5)$$

Applying the change of variables, $\tau_k = t_k - t_{k-1}$, and making the standard renewal process assumption of IEI independence enables the application of an IEI density function, such as that defined in Eq. 2. Recalling the assumption that events occur independently from cell to cell, we may formally state that $p_k^{(i)}\left(\tau_k^{(i)}\middle|\boldsymbol{\theta}_k^{(i)}\right) = p_0\left(\tau^{(i)}\middle|\boldsymbol{\theta}^{(i)}\right)$, for the kth event on the ith neuron.

In order to model asynchronous neural activity from the outset, we introduce a randomly distributed initial temporal offset, $t_0^{(i)}$, as one of the model parameters included in $\boldsymbol{\theta}^{(i)}$. Our model also assumes that inter-event intervals are centered around some value μ, unique for each neuron, so that $\mathcal{F}[p_0]$ can best be expressed as $\mathcal{F}[p_0] = e^{-i\mu\omega}\mathcal{F}[p_0']$. The quantity $\boldsymbol{\theta}$ is thus the n-tuple $[t_0,\mu]$, with $p(\boldsymbol{\theta}) = p_{t_0}(t_0)\ p_\mu(\mu)$.

The above assumptions imply that in general

$$\begin{aligned}\int df\ p(f)\,\mathcal{F}[f] &= \frac{1}{N_S}\mathcal{F}[p_{t_0}]\sum_{k=1}^{N_S}\left\{\left(\mathcal{F}\left[\sqrt{2\pi}p_0'\right]\right)^k \right.\\ &\quad \left.\times\,\mathcal{F}\left[\sqrt{2\pi}p_\mu\right](k\omega)\right\}, \quad (6)\end{aligned}$$

$$\begin{aligned}\int df\ p(f)\,|\mathcal{F}[f]|^2 &= \frac{1}{2\pi}\frac{1}{N_S}\left(1+\sum_{k=1}^{N_S-1}\left[2\left(\frac{N_S-k}{N_S}\right)\right.\right. \quad (7)\\ &\quad \left.\left.\times\,\mathrm{Re}\left\{\left(\mathcal{F}\left[\sqrt{2\pi}p_0'\right]\right)^k\mathcal{F}\left[\sqrt{2\pi}p_\mu\right](k\omega)\right\}\right]\right).\end{aligned}$$

In our specific model, Eq. 2 implies $p_0'(\tau) \sim \mathcal{N}(0,\sigma_{\text{jit}})$ and $p_\mu(\mu) \sim \mathcal{N}(\mu_0,\sigma_\mu)$. If we draw the initial temporal offsets from $p_{t_0}(t_0) \sim \text{unif}(-\mu_0/2,\mu_0/2)$, this yields

$$\int df\ p(f)\,\mathcal{F}[f] = \frac{1}{\sqrt{2\pi}}\frac{1}{N_S}\ \mathrm{sinc}\left(\frac{\mu_0\omega}{2}\right)\sum_{k=1}^{N_S} e^{-(k\sigma_{\text{jit}}^2+k^2\sigma_\mu^2)\omega^2/2}e^{-ik\mu_0\omega}, \quad (8)$$

$$\int df\ p(f)\,|\mathcal{F}[f]|^2 = \frac{1}{2\pi}\frac{1}{N_S}\left(1+\sum_{k=1}^{N_S-1}2\left(\frac{N_S-k}{N_S}\right)e^{-(k\sigma_{\text{jit}}^2+k^2\sigma_\mu^2)\omega^2/2}\cos(k\mu_0\omega)\right). \quad (9)$$

Note,

$$\left|\int df\ p(f)\,\mathcal{F}[f]\right|^2 = \frac{1}{N_S^2}\,\mathrm{sinc}^2\left(\frac{\mu_0\omega}{2}\right)\sum_{k=1}^{N_S}\left(e^{-(k\sigma_{\mathrm{jit}}^2+k^2\sigma_\mu^2)\omega^2} + 2\sum_{\ell=k+1}^{N_S}\cos\left((\ell-k)\mu_0\omega\right)e^{-((k+\ell)\sigma_{\mathrm{jit}}^2+(k^2+\ell^2)\sigma_\mu^2)\omega^2/2}\right).$$

Putting this together yields

$$\mathbb{E}_{p(f)}\left[|\mathcal{F}[f_T]|^2\right] = \frac{1}{2\pi}\frac{N_C}{N_S}\left(1+\sum_{k=1}^{N_S-1}2\left(\frac{N_S-k}{N_S}\right)\cos\left(k\mu_0\omega\right)e^{-(k\sigma_{\mathrm{jit}}^2+k^2\sigma_\mu^2)\omega^2/2}\right)$$
$$+\frac{1}{4\pi}\frac{N_C(N_C-1)}{N_S^2}\,\mathrm{sinc}^2\left(\frac{\mu_0\omega}{2}\right)\sum_{k=1}^{N_S}\left(e^{-(k\sigma_{\mathrm{jit}}^2+k^2\sigma_\mu^2)\omega^2} + 2\sum_{\ell=k+1}^{N_S}\cos\left((\ell-k)\mu_0\omega\right)e^{-((k+\ell)\sigma_{\mathrm{jit}}^2+(k^2+\ell^2)\sigma_\mu^2)\omega^2/2}\right). \quad (10)$$

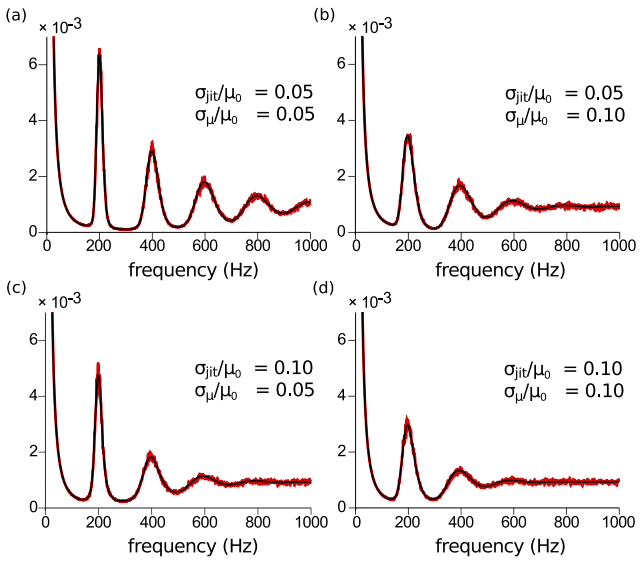

FIG. 1. Comparisons of analytically derived energy spectral density, Eq. 10 (black line), against numerically computed energy spectral density (red line). Note the excellent match between these results. Energy spectra are normalized over the range 10 to 1000 Hz. Each plot shown reflects the fixed parameters $\mu_0 = 5$ ms, $N_C = 500$ cells, and $N_S = 500$ spikes. Numerical results are averaged over 500 simulations.

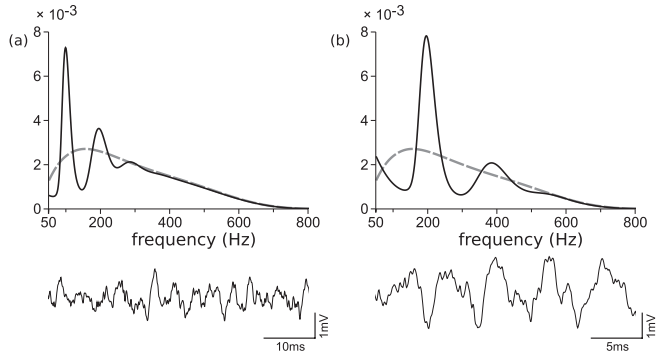

FIG. 2. Energy spectra (top) and example time-domain waveforms (bottom) for action potential (AP)-convolved model LFP signals. Spike time variability parameters were set to $\sigma_\mu/\mu_0 = 0.1$ and $\sigma_{\mathrm{jit}}/\mu_0 = 0.1$, with (a) $\mu_0 = 10$ ms and (b) $\mu_0 = 5$ ms. Normalized LFP energy spectra described by Eq. 10 (solid; black) were compared against the energy spectrum of the AP waveform (dashed; gray), which is also the energy spectrum of an AP-convolved Poisson process (white noise). Energy spectra were normalized to the range of 50 to 1000 Hz. Note stronger emergent rhythms with smaller μ_0 (higher frequency).

Eq. 10 is the final expression for the energy spectral density of the train of delta functions whose event times are specified by Eq. 2. Note that this result depends on five model parameters: N_S, the number of spikes per cell; N_C, the number of cells in the population; μ_0 and σ_μ, which together determine μ for each cell; and σ_{jit}, which introduces variability from event to event (i.e., "jitter"). Fig. 1 shows an excellent match between this analytical result and numerical simulations of the event train for several parameter combinations.

To make comparisons with experimental LFP recordings, the event train must be convolved with a realistic voltage waveform, resulting in the model LFP spectrum being the product of the event train spectrum and the waveform spectrum. Fig. 2 shows the results of convolving with a typical action potential (AP) waveform, for μ_0 corresponding to 100 Hz and 200 Hz. The model LFPs feature strong peaks in their spectra at both frequencies, and voltage traces from numerical simulations show a clear rhythm in the 200 Hz signal, demonstrating our primary point: completely asynchronous spiking may produce narrowband LFP rhythms when neural activity is quasi-periodic. The 100 Hz oscillation is not as obvious in the time domain because a large proportion of energy is concentrated as high-frequency noise at 300+ Hz.

Fig. 3 shows results from convolving the event train with a typical PSP waveform. Note how the energy of the PSP waveform is concentrated at much lower frequency than that of the AP waveform (gray dashed lines in Figs. 2 and 3), resulting in the 200 Hz PSP signal being severely attenuated compared to the 100 Hz PSP signal.

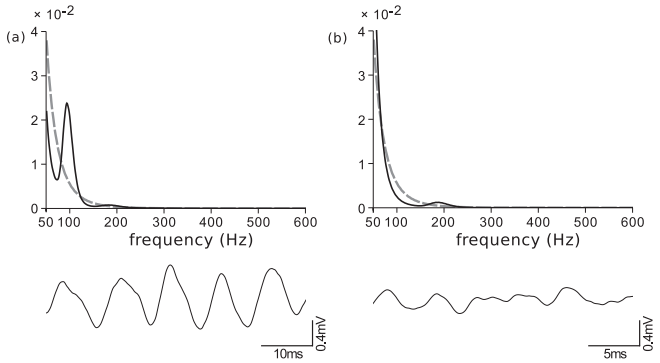

FIG. 3. Example energy spectra (top) and time-domain waveforms (bottom) for postsynaptic potential (PSP)-convolved model LFP signals. Parameters and normalization were set as in Fig. 2, with spectra of Eq. 10 (solid; black) compared against the spectrum of the PSP waveform (dashed; gray), which is also the energy spectrum of a PSP-convolved Poisson process (white noise). Note stronger emergent rhythms with larger μ_0 (lower frequency).

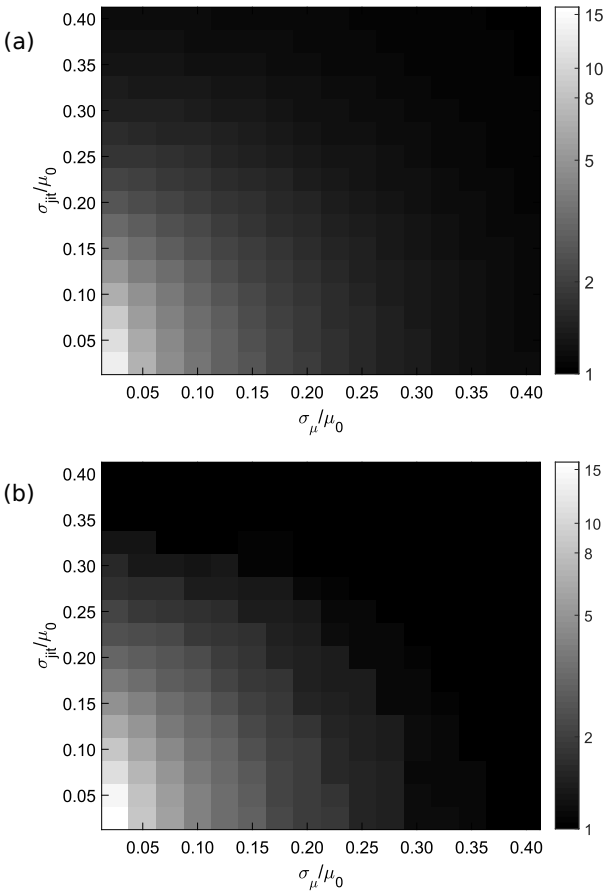

FIG. 4. Signal-to-noise ratio as function of spike time variability. (a) AP-convolved signal with $\mu_0 = 5$ ms. (b) PSP-convolved signal with $\mu_0 = 10$ ms. Note signal degradation is greater with increasing σ_μ/μ_0 against $\sigma_{\rm jit}/\mu_0$. Emergent rhythms depreciate beyond noticable detection when spike time variability ratios are each $\gtrsim 0.25$.

This provides a simple explanation for the conventional wisdom that PSPs tend to dominate the LFP at low frequency, while APs tend to dominate at higher frequency [9].

To characterize the strength of rhythms emerging from asynchronous neural activity, in Fig. 4 we plot the signal-to-noise ratio (SNR) as a function of σ_μ and $\sigma_{\rm jit}$ for 200 Hz AP-convolved LFPs and 100 Hz PSP-convolved LFPs. We define the SNR as the ratio of the LFP energy spectral density to the waveform energy spectral density at $f = \frac{1}{\mu_0}$. The waveform energy spectral density is considered the noise spectrum since it is what would result from a Poisson event train (white noise) convolved with the waveform. Note how σ_μ (population heterogeneity) and $\sigma_{\rm jit}$ (IEI heterogeneity) do not have the same effect on SNR—increasing σ_μ degrades SNR more quickly than increasing $\sigma_{\rm jit}$, as a result of its being attached to a factor of k^2 rather than k in Eq. 10. Our model therefore predicts that heterogeneity in mean firing frequency across a neural population will degrade asynchronous rhythms more than an equivalent degree of spike-time jitter. The results in Fig. 4 also suggest bounds on these two sources of spike-time variability for facilitating the emergence of LFP rhythms from asynchronous neural activity. For both AP events at 200 Hz and PSP events at 100 Hz, σ_μ and $\sigma_{\rm jit}$ can each reach as high as about 25% of μ_0 before the primary spectral peak is washed out by noise.

Our model therefore makes three main predictions. First, completely asynchronous and independent neural activity may produce robust, narrowband LFP oscillations, so long as individual neural activity is quasi-periodic. (Note that quasi-periodicity is essential—independent Poisson processes, for example, result in a flat power spectrum [10], but in many cases do not accurately describe neural activity [11, 12].) Previous computational work supports this hypothesis, suggesting that pathological "high-frequency oscillations" associated with epileptic seizures may be generated by a completely asynchronous, uncoupled network of hippocampal pyramidal cells receiving intense synaptic input [13]. Second, rhythms generated by asynchronous activity are degraded more by heterogeneity in intrinsic neuronal frequency than by neuronal jitter. And third, we have derived bounds on these two sources of heterogeneity for experimentally detecting oscillations from asynchronous neural activity. Our model additionally provides a simple mathematical explanation for why PSP waveforms tend to dominate the LFP at low frequency, while AP waveforms dominate at high frequency. These results should spur future experimental studies which investigate the possibility of neural oscillations emerging from asynchronous neural activity, especially under pathological conditions such as epileptic seizures.

This work was supported by NIH Grant Nos. R01-NS094399, K08-NS069783, UL1-TR000433, and K01-ES026839. We also acknowledge funding from the Doris Duke Charitable Foundation Career Development Award, NSF Grant No. 1003992, and the Ohio Wesleyan Summer Science Research Program. Special thanks to Bob Harmon for suggesting the helpful optics analogy.

* sgliske@umich.edu

[1] G. Buzsáki and A. Draguhn, Science **304**, 1926 (2004).
[2] X.-J. Wang, Physiological Reviews **90**, 1195 (2010).
[3] N. Brunel and X.-J. Wang, Journal of Neurophysiology **90**, 415 (2003).
[4] F. Moss, L. M. Ward, and W. G. Sannita, Clinical Neurophysiology **115**, 267 (2004).
[5] B. Doiron, B. Lindner, A. Longtin, L. Maler, and J. Bastian, Physical Review Letters **93**, 048101 (2004).
[6] C. Alvarado-Rojas, K. Lehongre, J. Bagdasaryan, A. Bragin, R. Staba, J. Engel Jr, V. Navarro, and M. Le Van Quyen, Frontiers in Computational Neuroscience **7** (2013).
[7] W. Truccolo, O. J. Ahmed, M. T. Harrison, E. N. Eskandar, G. R. Cosgrove, J. R. Madsen, A. S. Blum, N. S. Potter, L. R. Hochberg, and S. S. Cash, The Journal of Neuroscience **34**, 9927 (2014).
[8] B. Lindner, Physical Review E **73**, 022901 (2006).
[9] E. W. Schomburg, C. A. Anastassiou, G. Buzsáki, and C. Koch, The Journal of Neuroscience **32**, 11798 (2012).
[10] A. Papoulis and S. U. Pillai, *Probability, Random Variables, and Stochastic Processes* (McGraw-Hill, New York, New York, 1984).
[11] A. D. Reyes, Nature Neuroscience **6**, 593 (2003).
[12] H. Câteau and A. D. Reyes, Physical Review Letters **96**, 058101 (2006).
[13] C. G. Fink, S. Gliske, N. Catoni, and W. C. Stacey, eNeuro **2**, ENEURO (2015).